

Anomalous Magnetic Depolarization of Fluorescence from the NO_2 2B_2 State

H. FIGGER,¹ D. L. MONTS,² AND R. N. ZARE³

Department of Chemistry, Columbia University, New York, New York 10027

Hanle-effect studies were made of 13 identified lines belonging to the 5933-, 6117-, 6125-, and 6126-Å bands of the NO_2 2B_2 state. The fluorescence was excited using a tunable cw dye laser operated single mode, using NO_2 pressures as low as 0.2 mTorr. From the variation of the fluorescence intensity with magnetic field the product $g\tau_C$ is deduced, where g and τ_C are the excited state g value and coherence lifetime, respectively. Using previously determined radiative lifetimes, g is obtained and compared to the values of g expected from Hund's case (*b*) coupling. The observed g values do not display the expected N' dependence and are about an order of magnitude smaller than predicted. An alternative explanation is that the g values are behaved, but the coherence lifetime is shorter than the radiative lifetime, caused by radiationless dephasing processes which may be collisional or intrinsic.

I. INTRODUCTION

The depolarization of resonance fluorescence by the application of an external magnetic field was first observed by Hanle (*1*) more than 50 years ago. Since then, Hanle-effect studies and other investigations depending on interference effects in coherently prepared excited states have been extensively exploited in atomic spectroscopy (*2*), but these possibilities are only beginning to be realized in molecular structure studies (*3*). Because the Hanle effect permits resolution limited by the natural width rather than the Doppler width of a line, its application to the complex spectra of molecules is appealing. Although a number of diatomic systems have been investigated, observations of the Hanle effect in triatomics have been restricted to CS_2 (*4*), SO_2 (*5*), NH_2 (*6*), and NO_2 (*7*), for which studies have been made of resolved fluorescence on only the latter two.

We report here Hanle-effect measurements of some selected lines of the NO_2 visible spectrum. The NO_2 molecule was chosen because its spectrum is notorious for appearing extensively perturbed by what is believed to be interaction of the upper state levels with high vibrational levels of the ground state (*8*). Since the classical Zeeman studies of Fortrat (*9*), it has been recognized that perturbed lines in a molecular spectrum show a more sensitive dependence on magnetic field than neighboring normal lines in the same band. The reason for this is that the magnetic field "disturbs" the levels that perturb one another. If the Zeeman splitting of the perturbed state is different from that of the

¹ Present address: MPG Projektgruppe für Laserforschung, D-8046, Garching bei München, Germany.

² Present address: Department of Chemistry, Rice University, Houston, Tex. 77001.

³ Present address: Department of Chemistry, Stanford University, Stanford, Calif. 94305.

perturbing state, then the interaction causing the perturbation between individual magnetic sublevels (M components) will vary strongly with applied magnetic field. It is hoped that measurements of this variation will provide insight into the nature of the perturbation. Perhaps it is not surprising then that we find that the magnetic depolarization of NO₂ resonance fluorescence behaves anomalously, in a manner not previously observed in other molecular excited states. These first measurements of this type encourage us that the Hanle effect provides an interesting "window" on the perturbed NO₂ visible spectrum.

II. EXPERIMENTAL METHOD

Figure 1 shows the experimental setup. A 22-cm-diameter spherical bulb contains NO₂ at a pressure of 0.5 to 100 mTorr, as measured with a capacitance manometer. This fluorescence cell is illuminated by a cw dye laser beam, defined to travel along the x axis. The light beam is linearly polarized with its electric vector defined to point along the y axis. A variable magnetic field is applied along the z axis. The NO₂ fluorescence is detected by a photomultiplier positioned along the y axis. Between the NO₂ sample and the photomultiplier is a linear polarizer which only transmits light polarized along the x axis. The magnetic field is modulated and the variation of the fluorescence intensity with magnetic field is measured using a lock-in amplifier. This procedure yields a derivative signal, characterized by a half-width, ΔH . By extrapolating to zero modulation field, to zero NO₂ pressure, and to zero laser power, the quantity $H_{\frac{1}{2}}^0$, corresponding to the HWHM of a Lorentzian, is obtained.

Simple theory (3) shows that for a quantum mechanical system in a sharp angular momentum state J , the zero-field level crossing signal (Hanle effect) relates the coherence lifetime τ_C and the separation $\Delta E(M, M')$ between the coherently excited magnetic

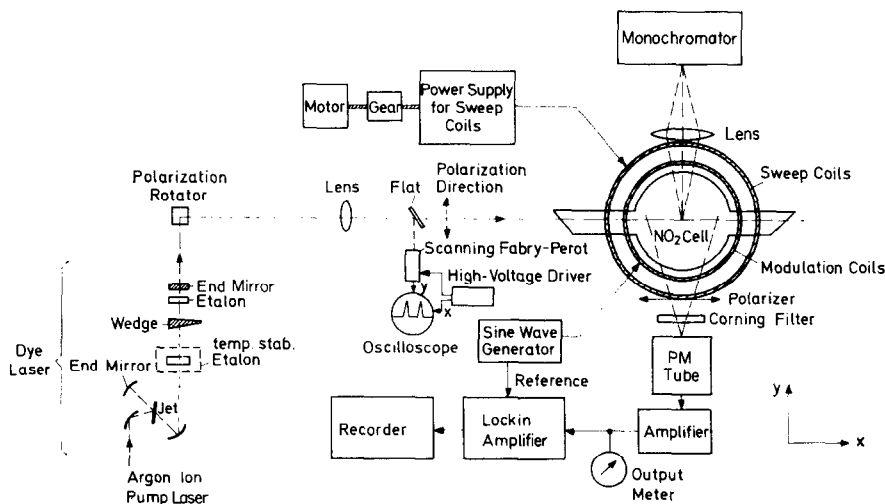


Fig. 1. Schematic of the experimental setup. The Helmholtz coils for compensation of the x - and y -components of the Earth's magnetic field are omitted here. The cw dye laser on the left-hand side has to be thought of as rotated by 90° around its long axis to give the polarization discussed in the text.

sublevels M and M' at the field strength H_1^0 to one another by

$$\Delta E(M, M')\tau_C = \hbar, \quad (1)$$

where \hbar is Planck's constant divided by 2π . Using linearly polarized light and the right-angle excitation-detection geometry of Fig. 1, only $M' = M \pm 2$ sublevels can be coherently excited. Thus

$$\Delta E(M, M') = 2g\mu_0 H_1^0, \quad (2)$$

where μ_0 is the electronic Bohr magneton and g is the Landé factor. Hence for such a system, a measurement of H_1^0 permits the determination of the product $g\tau_C$ from the relation

$$g\tau_C = \hbar / (2\mu_0 H_1^0). \quad (3)$$

In the limit of no collisions, the coherence lifetime τ_C is assumed to be equal to the radiative lifetime τ_R . If τ_R is known from prior lifetime measurements, then the Hanle effect provides a determination of the magnetic moment of the excited state. We describe here the procedure for determining H_1^0 .

A. Magnetic Field

The magnetic field is generated by a pair of 1-m-diameter Helmholtz coils. At 100-mG field strength the inhomogeneity is typically 1 mG/cm in the center of the fluorescence cell. The x and y components of the earth's field are canceled by two additional pairs of Helmholtz coils; the z component of the earth's field (approximately 0.2 G) adds to the variable magnetic field H . All magnetic field measurements are performed using a Hall-probe gaussmeter (Bell Model 640), which has been calibrated against a rubidium magnetometer. A search proved negative for the presence of low frequency (≤ 1 kHz) ac magnetic fields in the region of the fluorescence cell.

B. Detection System

The photomultiplier (Bailey 4283 SA-25 photocathode) views the NO_2 fluorescence cell through a red filter (Corning CS2-58) and a linear polarizer (Vivitar). The filter transmits wavelengths only beyond 6200 Å, and suppresses light at the laser wavelength by a factor of 10^4 . No scattered laser light is detected above the noise level. The linear polarizer is oriented to transmit fluorescence with its electric vector parallel to the x axis.

Because of the long radiative lifetime of the excited NO_2 molecule, a correction must be made for those excited molecules that drift from the field of view before emitting fluorescence. To estimate the magnitude of the effect, the following experiment was performed. The output of the photomultiplier was recorded as a small light source was moved in the xz plane. The signal is flat for small deviations from the y axis, falling by only 10% of its value at the center for the location of the light source 4 cm from the y axis. However, beyond this excursion the falloff is rapid, the 50% value being at 6 cm. If we assume that all molecules are viewed with the same response up to 6-cm excursions from the y axis, and no molecules can be observed beyond this circle, then there is a small reduction in the apparent lifetime, amounting to only 3% for a 75- μ sec lifetime (10). This error, although systematic, is smaller than other errors, and therefore no correction is made.

The photomultiplier is magnetically shielded but it is not cooled. The signal is amplified and then fed into a lock-in detector (Princeton Applied Research Model HR8 with type A preamplifier) operated with a 3-sec time constant. Phase sensitive detection is used because the magnitude of the signal is comparable to the intensity fluctuations (2-5%) of the cw dye laser. A sine-wave generator (Kronhite Model 4200) causes the magnetic field H to be modulated at 70-200 Hz. This is accomplished by a pair of Helmholtz coils, 32 cm in diameter, nested inside the larger Helmholtz sweep coils. Higher frequencies would have been desirable to eliminate more completely the laser intensity fluctuations, but could not be used because of the inductance of the modulation coils. The lock-in output drives an XY recorder when the magnetic field is swept by an operational amplifier (Kepco Model CK 18-3M). The voltage output of the latter is controlled by a precision motor. The scan rate is typically 5 mG/sec and the Hanle effect is recorded in 2 to 3 min. The XY recorder is linear to better than $\pm 1\%$ for a given scan.

C. NO₂ Cell

The fluorescence cell is the same as that used previously (11, 12). It is a 22-cm Pyrex bulb with entrance and exit arms terminating in Brewster's angle windows, evacuated by an oil diffusion pump, backed by a rotary mechanical pump separated from the diffusion pump by a liquid nitrogen trap. A capacitance manometer measures the pressure in the cell. Purified NO₂ is stored in a cold finger. First the NO₂ sample is cooled to liquid nitrogen temperatures and volatile impurities are pumped away. Then, the cold finger is warmed, admitting NO₂ into the main fluorescence cell. Gas samples are changed every few hours. This is necessary because it was noted that the laser light caused some photochemical reaction to occur upon continued exposure.

D. Excitation Source

The NO₂ fluorescence is excited by a tunable cw dye jet laser (Spectra-Physics Model 375 with Model 581A etalon). The active medium is rhodamine 6G dissolved in ethylene glycol. It is pumped by a 4-W argon ion laser operating on all lines (Spectra-Physics Model 165). The dye laser employs the folded three-mirror cavity design which compensates for astigmatism (13).

The frequency-selective elements inside the dye laser cavity are a wedged interference filter, a 0.1-mm-thick etalon, and a 2-mm air-spaced temperature-stabilized etalon, which selects a single longitudinal cavity mode.

The spacing of the two reflectors of the 2-mm etalon is varied piezoelectrically, making the laser wavelength jump between adjacent longitudinal modes, spaced about 500 MHz apart. Since the NO₂ Doppler width is about 1.5 GHz at room temperature, it is possible to tune to a single NO₂ absorption line by hopping from one mode to the next. The exact tuning to the center of the line is achieved by moving piezoelectrically the flat end mirror. The mode structure of the dye laser output is monitored with a scanning Fabry-Perot interferometer (Spectra-Physics Model 470-4). The width of a single mode is measured to be about 50 MHz when the bench upon which the pump laser and dye laser rests has no special vibration damping.

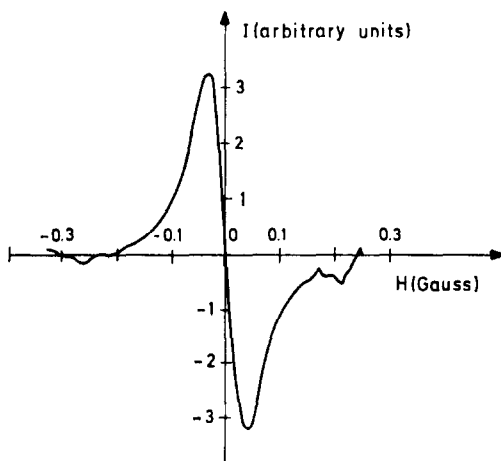


FIG. 2. Hanle curve for the $N' = 13$, $K'_a = 1$ line at $6127.59\text{-}\text{\AA}$. Here the modulation amplitude was $H_{\text{mod}} = 0.3 H_1$. The pressure in the cell was 0.6 mTorr. This trace was recorded in 2 to 3 min.

When the laser operates on a single longitudinal mode, the intensity fluctuation is found to be 2 to 5%, as observed on an oscilloscope which monitors the output of the scanning Fabry-Perot interferometer. Under these conditions, the maximum power, as measured by an Eppley power meter, is about 100 mW at 5933 \AA and about 50 mW at 6125 \AA when the argon ion pump laser has an output power of 4.5 W.

Usually the laser remains in the same mode for about 10 min. Then the air-spaced etalon must be readjusted to compensate for hopping into an adjacent mode. However, this stability is sufficient to permit a scan of the Hanle effect.

By using a lens, the divergent laser beam is made almost parallel before it enters the NO_2 cell. The beam diameter is about 1 cm and the polarization vector is rotated by two 90° prisms so that it is in the horizontal plane. This prism setup also facilitated the adjustment of the beam height in the cell.

E. Measurement Procedure

The Hanle effect is observed for selected NO_2 absorption lines. The lines were chosen to satisfy two criteria: (1) the lifetime of the upper state of the transition should have been measured or estimated previously;⁴ (2) the quantum numbers of the transition should have been assigned previously (11, 12).

Based on these criteria, the Hanle effect of 13 NO_2 lines belonging to four different bands situated around 5933 , 6117 , 6125 , and 6126 \AA , were recorded.

⁴ The lifetimes were determined using one of two procedures. In each case, the NO_2 is contained in a 33-cm-diameter bulb at a pressure ≤ 1 mTorr, and the fluorescence is excited by a flashlamp-pumped tunable dye laser sufficiently narrow (0.03 \AA) to excite individual transitions. In the first procedure, the lifetime is determined as the average of the lifetime obtained from photographs of oscilloscope decay traces following a single laser pulse. In the second procedure, the lifetime is determined as the average of the lifetimes obtained from the output of a scanning boxcar integrator. Within experimental error, the lifetimes obtained from photographs and from boxcar averaging were identical.

Before each run, a Spex 1-m monochromator (see Fig. 1) is set to the wavelength of the desired NO₂ line with the help of nearby calibration lines of Ne, Hg, Cd, or Th. In this manner, the laser could be tuned to within 0.02 Å of the absorption line. Fine tuning is achieved by maximizing the fluorescence. In each case, the dispersed NO₂ fluorescence is checked in order to confirm the identity of the transition. This procedure typically takes about an hour, after which the NO₂ sample is pumped away and then refilled.

The Hanle effect is first recorded with relatively high strengths of the modulation field, i.e., the modulation amplitude is comparable to the width of the Hanle curve. The modulation field is then reduced until the Hanle width becomes essentially constant. Figure 2 shows a typical trace of the Hanle effect. The theory of a modulation-broadened Lorentzian curve shows that the extrema, H_{\pm} , appear as a function of the modulation field at

$$H_{\pm} = \pm 3^{-1/2} H_{1/2} \{ [4 + 3(H_{\text{mod}}/H_{1/2})^2]^{1/2} - 1 \}, \quad (4)$$

where H_{mod} is the modulation field and $H_{1/2}$ the HWHM of the Lorentzian curve (14). The values of H_{\pm} are determined graphically from the recorded Hanle curves with an estimated error of $\pm 10\%$. Equation (4) is found to be satisfied experimentally to within our uncertainty. Using Eq. (4), the value of $H_{1/2}$ in the limit of zero modulation field is determined from the relation

$$H_{1/2} = \frac{1}{2} 3^{1/2} (H_{+} - H_{-}). \quad (5)$$

Then a short extrapolation of $H_{1/2}$ values as a function of H_{mod} is made.

In addition to extrapolating to zero modulation broadening, the power density of the laser beam is varied to learn its effect. It is possible that optical pumping of the ground state causes distortion. To test for this, the lens was removed from the beam path (see Fig. 1). This enlarged the beam cross section by a factor of 6 and correspondingly reduced the power density. Then the laser power was varied between 5 and 50 mW. The shapes and widths of the Hanle curves are not altered outside of experimental error.

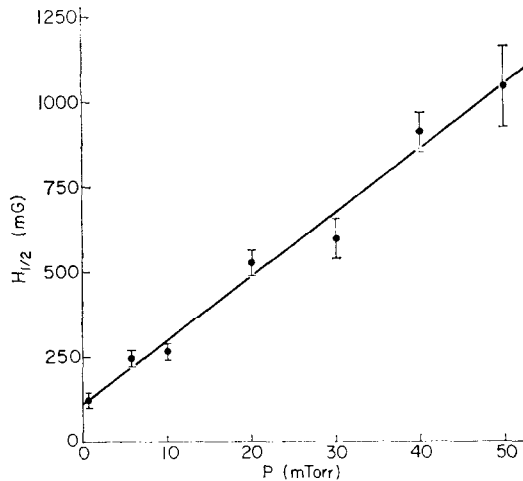


FIG. 3. Plot of $H_{1/2}$ versus pressure for the $N' = 6$, $K'_a = 1$ line of 6128.44-Å. The straight line is a weighted least-squares fit to the measured values which we indicate as circles with error bars.

The width of the Hanle curve depends on the density of the scattering gas. The coherence lifetime, τ_C , can be lengthened by radiation trapping, causing the Hanle curve to narrow. On the other hand, collisions may shorten the coherence lifetime, causing the Hanle curve to broaden. For molecular systems, radiation imprisonment is usually not severe even at high pressures, since only a small fraction of the total fluorescence can be reabsorbed. However, the collisional destruction of coherence can be significant. The process may be described by

$$1/\tau_C = (1/\tau_R) + n\langle v\sigma_C \rangle, \quad (6)$$

where τ_R is the radiative lifetime, n is the density of the molecular scatterers, σ_C is the coherence (alignment) destruction cross section, and v is the relative velocity of the collision partners. For all lines investigated, the Hanle effect is recorded as a function of NO_2 pressure in the fluorescence cell (see Fig. 3). The pressure is reduced from about 100 to 0.5 mTorr in five to eight steps. As expected, the Hanle signal is found to be broadened linearly with pressure, at pressures typically 30 mTorr and less. At pressures lower than about 0.2 mTorr, the signal becomes lost in the noise. The extrapolation of $H_{\frac{1}{2}}$ to zero pressure yields $H_{\frac{1}{2}}^0$.

In order to ensure that the effect we observe is not spurious, such as the effect of the magnetic field on the photomultiplier gain, experiments were performed with the polarization vector of the light directed along the z axis. Under these conditions, the magnetic sublevels cannot be coherently excited, and the Hanle signal is observed to disappear into the noise.

III. RESULTS AND DISCUSSION

Table I presents the results of our Hanle-effect studies. The first four columns identify the 13 excited state levels investigated. Column 5 lists the values of $H_{\frac{1}{2}}^0$, the half-width at half-maximum of the Lorentzian curve obtained by extrapolating both the modula-

TABLE I
Hanle-Effect Data for Selected NO_2 Transitions

Band (\AA)	λ (\AA)	N'	K'_a	$H_{1/2}^0$ (mG)	$q\tau_C$ (10^{-7} sec)	S (mG/mTorr)
5933	5934.41	3	0	27*15	21*12	5.5*2.0
5933	5934.47	3	0	42*15	13*5	2.1*0.9
5933	5934.53	3	1	45*3	13*1	0.92*0.22
5933	5939.17	15	0	75*12	7.6*12	7.2*2.7
6117	6110.88	17	0	52*5	11*1	18*1
6117	6110.95	17	1	65*14	8.8*1.9	18*2
6117	6111.05	17	1	62*12	9.1*1.7	22*2
6125	6121.62	7	1	78*5	7.3*0.4	18*1
6125	6127.59	13	1	52*2	11*1	12*1
6125	6114.11	22	1	60*6	9.5*0.9	19*2
6126	6127.48	3	1	88*5	6.5*0.4	2.2*0.8
6126	6128.44	6	1	55*13	10*3	9.6*0.9
6126	6129.16	8	1	64*6	9.0*0.9	7.0*1.2

Uncertainty of $H_{\frac{1}{2}}^0$ and S is based on 70% confidence limits.

TABLE II

Analysis of the Hanle-Effect Data Assuming $\tau_C = \tau_R$

Band (Å)	λ (Å)	N'	K'_a	τ_R (μ sec) ^o	g derived ^o	$g(J')$
5933	5934.41	3	0	87 ± 9 (19 ± 2)	0.025 ± 0.016 (0.11 ± 0.08)	0.2860
5933	5934.47	3	0	100 ± 15 ^c (25 ± 5) ^c	0.013 ± 0.007 (0.054 ± 0.029)	0.2860
5933	5934.53	3	1	100 ± 15 ^c (25 ± 5) ^c	0.013 ± 0.003 (0.050 ± 0.013)	0.2860
5933	5939.17	15	0	100 ± 15 ^c (25 ± 5) ^c	0.0076 ± 0.0024 (0.031 ± 0.011)	0.0646
6117	6110.88	17	0	60 ± 6 ^d	0.018 ± 0.004	0.0572
6117	6110.95	17	1	57 ± 1	0.015 ± 0.004	0.0572
6117	6111.05	17	1	57 ± 1	0.016 ± 0.003	0.0572
6125	6121.62	7	1	65.5 ± 6	0.011 ± 0.002	0.1335
6125	6127.59	13	1	75 ± 7 ⁱ	0.015 ± 0.002	0.0741
6125	6114.11	22	1	75 ± 7 ⁱ	0.013 ± 0.002	0.0445
6126	6127.48	3	1	75 ± 7 ⁱ	0.0086 ± 0.0013	0.2860
6126	6128.44	6	1	75 ± 7 ⁱ	0.014 ± 0.005	0.1540
6126	6129.16	8	1	75 ± 7 ^h	0.012 ± 0.002	0.1178

^oIn the case of the 5933 Å band, there is some ambiguity because the radiative decay appears to be bi-exponential (15). We have taken the longer lifetime as the coherence lifetime, since this makes the behavior of this band similar to the others. We present in parentheses the alternative choice of lifetime and resulting g value.

^hEstimated lifetime based on lifetimes of nearby transitions of the same vibronic band.

tion broadening and the pressure to zero. With these $H_{\frac{1}{2}}^0$, we obtain $g\tau_C$ (column 6) using Eq. (3). The last column lists the values for the collisional destruction of coherence, reported as mG/mTorr. These values are found from the slopes, S , of the $H_{\frac{1}{2}}$ versus pressure plots.

Our first attempt to analyze the data presented in Table I was to assume that $\tau_C = \tau_R$ and hence to derive g values from $H_{\frac{1}{2}}^0$. The results of this analysis are shown in Table II. The ²B₂ electronic state of NO₂ is bent. Therefore, the electronic angular momentum is quenched, i.e., is not a constant of the motion. The electron spin, $S' = \frac{1}{2}$, is coupled to the rotational angular momentum N' to form the total angular momentum J' (disregarding nuclear spin I'). For such a coupling scheme, called Hund's case (b), the g values are calculated to be (16)

$$g(J') = \pm 1.001 / (N' + \frac{1}{2}), \quad (7)$$

where $J' = N' \pm \frac{1}{2}$. For $J' \gg I'$, these g values are only slightly altered by the presence of hyperfine structure. We have listed in column 7 of Table II the g values expected from this simple theory [Eq. (7)].

We see at once that there is no agreement between these g values and those derived from our measurements (column 6). The latter are smaller, typically by more than a factor of 5, and appear to be internally consistent. Moreover, in the 6125- and 6126-Å bands, g does not decrease with N' as Eq. (7) predicts. Instead, the $g\tau_C$ values versus N' appear to be almost independent of N' , as seen in Fig. 4. Although our $g\tau_C$ values show scatter, we feel confident that we have eliminated all effects that could distort our Hanle curves to such an extent so as to cause the disagreement between $g(J')$ and the experimentally derived g value.

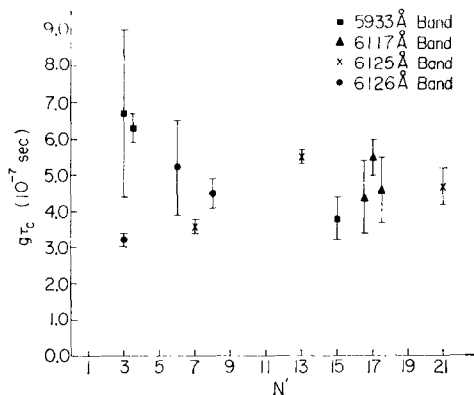


FIG. 4. Plot of the experimentally derived $g\tau_C$ values versus N' . The $g\tau_C$ of the 5934.41-Å transition is not included in this plot.

There is additional evidence that the $g\tau_C$ values obtained from Hanle effect studies of NO_2 are anomalous. Prior to this work, Wallace (7) used a pulse dye laser and gated detection electronics to study in this laboratory some selected levels of the NO_2 5933-Å band. His results are in fair agreement with those reported here. For example, his value of H_3^0 for the 5934.41-Å transition is 48 ± 6 mG,⁵ compared to our value of 27 ± 15 mG. Our values for the other two $N' = 3$ transitions of the 5933-Å band investigated are about 45 mG.

Recently, Bonilla and Demtröder (17) have measured Hanle widths using various lines of the argon ion laser as the excitation source. Again, values of H_3^0 were found that were anomalous in that they were much wider than expected from the product of the theoretical g value and the radiative lifetime.

An alternative interpretation suggested to us by Miller (18) is to abandon the assumption that $\tau_C = \tau_R$ and assume instead that g is well behaved, i.e., given by Eq. (7). This treatment yields the coherence lifetime, τ_C , and the coherence destruction cross section, σ_C , listed in Table III. We find that τ_C is much less than τ_R , while σ_C is approximately 90 \AA^2 in most cases. We find that this treatment leads to a rather consistent interpretation. This way of analyzing the data is also favored by Demtröder (19). Indeed, if we fix $\sigma_C = 90 \text{ \AA}^2$, then the g values calculated from the experimental measurements of H_3^0 and τ_R are in good agreement (see column 7 of Table III) with the $g(J')$ values given by Eq. (7).

Finally, we must confront the question of what causes τ_C to be less than τ_R . One possible explanation is that the origin of this effect is collisional, even though H_3 has been extrapolated to zero pressure. For the $90\text{-}\text{\AA}^2$ coherence destruction cross section, the mean time between collisions is about $30 \mu\text{sec}$ at 0.5 mTorr. For one collision every microsecond at this pressure, the cross section must be almost 3000 \AA^2 . Thus this interpretation leads us to a contradiction in that $\sigma_C \approx 90 \text{ \AA}^2$ gives a consistent set of g values while the coherence destruction cross section must be at least an order of magnitude larger to account for $\tau_C \ll \tau_R$.

⁵ In his thesis, Wallace gives H_3^0 as 95 ± 12 mG; however, H_3^0 is defined as FWHM rather than HWHM.

TABLE III

Analysis of the Hanle-Effect Data Assuming the g Value is Well Behaved

Band (Å)	λ (Å)	N'	K'_a	τ_c (μ sec)	σ_c (10^{-15} cm ²)	g ($\sigma = 90\text{Å}^2$)	g (J')
5933	5934.41	3	0	7.4 ± 4.2	$20^{+4.1}_{-2.6}$ ($13^{+3.2}_{-2.2}$)	$0.15^{+0.31}_{-0.20}$ ($0.23^{+0.50}_{-0.32}$)	0.2860
5933	5934.47	3	0	4.7 ± 1.6	$79^{+14.2}_{-7.3}$ ($6.8^{+12.8}_{-6.9}$)	$0.32^{+0.62}_{-0.34}$ ($0.36^{+0.71}_{-0.40}$)	0.2860
5933	5934.53	3	1	4.4 ± 0.3	$3.4^{+1.6}_{-1.1}$ ($3.0^{+1.5}_{-1.0}$)	$0.73^{+0.44}_{-0.33}$ ($0.77^{+0.50}_{-0.38}$)	0.2860
5933	5939.17	15	0	1.2 ± 2	$5.5^{+5.8}_{-3.3}$ ($3.3^{+4.4}_{-2.9}$)	$0.10^{+0.12}_{-0.07}$ ($0.12^{+0.15}_{-0.09}$)	0.0646
6117	6110.88	17	0	1.9 ± 2	$9.5^{+3.5}_{-3.2}$	$0.055^{+0.021}_{-0.019}$	0.0572
6117	6110.95	17	1	1.5 ± 3	$99^{+6.5}_{-5.9}$	$0.053^{+0.031}_{-0.028}$	0.0572
6117	6111.05	17	1	1.6 ± 3	12^{+7}_{-6}	$0.047^{+0.022}_{-0.021}$	0.0572
6125	6121.62	7	1	5.5 ± 0.3	30 ± 6	0.048 ± 0.013	0.1335
6125	6127.59	13	1	1.5 ± 1	$98^{+1.7}_{-1.6}$	0.069 ± 0.016	0.0741
6125	6114.11	22	1	2.1 ± 2	$83^{+3.2}_{-2.9}$	$0.047^{+0.019}_{-0.017}$	0.0445
6126	6127.48	3	1	2.3 ± 0.1	$81^{+5.8}_{-3.0}$	$0.32^{+0.25}_{-0.14}$	0.2860
6126	6128.44	6	1	6.7 ± 1.6	$18^{+1.2}_{-1.1}$	$0.083^{+0.059}_{-0.054}$	0.1540
6126	6129.16	8	1	7.6 ± 0.7	10 ± 4	$0.11^{+0.06}_{-0.05}$	0.1178

*See Footnote a in Table II.

Another possible explanation is that the origin of this effect is intrinsic, i.e., it arises from intramolecular radiationless dephasing. In this picture the molecule "hops" to nearby levels of the same total angular momentum, F , but with different $g(F')$ values. It is tempting then to associate τ_c with the lifetime calculated from integrated absorption measurements. Neuberger and Duncan (20) reported an integrated absorption coefficient lifetime of 0.26 μ sec. Donnelly and Kaufman (21) have reexamined Neuberger and Duncan's work and have calculated a lifetime of ~ 1.5 μ sec at 5930 Å. More recently, Donnelly and Kaufman (22) have discovered that when the fluorescence spectrum is corrected for detector response and is plotted in constant wavenumber units, the fluorescent intensity increases to the red as far as they were able to follow it (7300 cm⁻¹ below the excitation frequency). This further lengthens the estimated integrated absorption coefficient lifetime by about a factor of 5. Thus, τ_c and the integrated absorption lifetime are of the same order of magnitude. However, the calculated density of appropriate levels may be too low to support this interpretation.

It appears then that objections can be made to both explanations. To further our understanding of this phenomenon, it is suggested that additional experiments be performed. In particular, it would be valuable to have independent measurements of the g values, e.g., by double resonance, as well as τ_c values, e.g., by the measurement of the homogeneous linewidth by double resonance spectroscopy (23) or by other means

(24). In closing, it may be that the origin of the anomalous magnetic depolarization of NO_2 fluorescence (0–0.5 G) reported here is related to the anomalous magnetic quenching of NO_2 fluorescence (0–17.7 kG) reported by Butler and Levy (25). In their experiments the magnetic quenching cross section is an erratic function of the excitation wavelength, appears to grow with increasing magnetic field, and could be explained once again by radiationless processes which are collisional and/or intrinsic.

ACKNOWLEDGMENTS

We have benefited from provocative conversations with W. Demtröder, T. A. Miller, and R. Wallace. We are also grateful to C. Denise Caldwell for calibrating the Bell gaussmeter. One of us (H.F.) thanks the Deutsche Forschungsgemeinschaft (DFG), for a fellowship. Support from the National Science Foundation under Grant No. NSF-CHE75-22338 is gratefully acknowledged.

RECEIVED: June 2, 1977

REFERENCES

1. W. HANLE, *Z. Phys.* **30**, 93 (1924).
2. W. HAPPER, *Rev. Mod. Phys.* **44**, 169 (1972).
3. R. N. ZARE, *Colloq. Int. Cent. Nat. Rech. Sci.* **217**, 29 (1973); *Accounts Chem. Res.* **4**, 361 (1971); *J. Chem. Phys.* **45**, 4510 (1966).
4. S. J. SILVERS AND M. R. MCKEEVER, *Chem. Phys.* **18**, 333 (1976); J. W. MILLS AND R. N. ZARE, *Chem. Phys. Lett.* **5**, 37 (1970).
5. H. M. POLAND AND R. N. ZARE, *Bull. Amer. Phys. Soc.* **15**, 347 (1970).
6. M. KROLL, *J. Chem. Phys.* **63**, 1803 (1975).
7. R. WALLACE, Ph.D. Thesis, Columbia University, 1977; 30th Symposium on Molecular Structure and Spectroscopy, Columbus, Ohio, June 16–20, 1975, Book of Abstracts, MG4.
8. A. E. DOUGLAS, *J. Chem. Phys.* **45**, 1007 (1966).
9. R. FORTRAT, *Ann. Phys. (Paris)* **3**, 345 (1915); *C. R. Acad. Sci. (Paris)* **156**, 1459 (1913).
10. P. B. SACKETT AND J. T. YARDLEY, *J. Chem. Phys.* **57**, 152 (1972).
11. C. G. STEVENS AND R. N. ZARE, *J. Mol. Spectrosc.* **56**, 167 (1975).
12. D. L. MONTS, B. SOEP, AND R. N. ZARE, *J. Mol. Spectrosc.*, to appear.
13. H. KOGELNIK, E. P. IPPEN, A. DIENES, AND C. V. SHANK, *IEEE J. Quant. Electron.* **QE-8**, 1373 (1972).
14. R. ARNDT, *J. Appl. Phys.* **36**, 2522 (1965); G. W. SMITH, *J. Appl. Phys.* **35**, 1217 (1964); H. WAHLQUIST, *J. Chem. Phys.* **35**, 1708 (1961); K. HALBACH, *Phys. Rev.* **119**, 1230 (1960).
15. C. G. STEVENS, M. SWAGEL, R. WALLACE, AND R. N. ZARE, *Chem. Phys. Lett.* **18**, 465 (1973).
16. F. H. CRAWFORD, *Rev. Mod. Phys.* **6**, 90 (1934).
17. I. R. BONILLA AND W. DEMTRÖDER, *Chem. Phys. Lett.*, to appear.
18. T. A. MILLER, private communication.
19. W. DEMTRÖDER, private communication.
20. D. NEUBERGER AND A. B. F. DUNCAN, *J. Chem. Phys.* **22**, 1693 (1954).
21. V. M. DONNELLY AND F. KAUFMAN, *J. Chem. Phys.* **66**, 4100 (1977).
22. V. M. DONNELLY AND F. KAUFMAN, *J. Chem. Phys.*, to appear.
23. R. SOLARZ AND D. H. LEVY, *J. Chem. Phys.* **60**, 842 (1974).
24. R. G. BREWER AND A. Z. GENACK, *Phys. Rev. Lett.* **36**, 959 (1976); A. H. ZEWAHL, T. E. ORLOWSKI, AND D. R. DAWSON, *Chem. Phys. Lett.* **44**, 379 (1976).
25. S. BUTLER AND D. H. LEVY, *J. Chem. Phys.* **66**, 3538 (1977).